The crystal structure, magnetic susceptibility, electrical resistivity, specific heat, and electronic band structure of RAuGe (R = Sc, Y, La, Lu)

1997 J. Phys.: Condens. Matter 9 1435

(http://iopscience.iop.org/0953-8984/9/7/009)

J. Phys.: Condens. Matter **9** (1997) 1435–1450. Printed in the UK PII: S0953-8984(97)79645-0

The crystal structure, magnetic susceptibility, electrical resistivity, specific heat, and electronic band structure of RAuGe (R = Sc, Y, La, Lu)

W Schnelle, R Pöttgen†, R K Kremer, E Gmelin and O Jepsen
Max-Planck-Institut für Festkörperforschung, Heisenbergstraße 1, D-70569 Stuttgart, Germany

Received 18 November 1996

Abstract. The title compounds were prepared by arc melting of the elements and subsequent annealing. Their structures were refined from single-crystal x-ray diffractometer data. While YAuGe and LaAuGe adopt the structure of NdPtSb, the structures of ScAuGe and LuAuGe are more closely related to that of LiGaGe. The crystal chemistry of these germanides is briefly discussed. The four compounds are weak diamagnets. The ratios of their Pauli susceptibilities and their electronic specific heat coefficients are the same for the Y, La, and Lu compounds. The electrical resistivities of ScAuGe and LuAuGe are metal-like (60/90 $\mu\Omega$ cm), while YAuGe and especially LaAuGe show much higher resistivities which saturate at high temperatures (800 $\mu\Omega$ cm for LaAuGe at 300 K). The electronic properties of the four compounds are discussed on the basis of TB-LMTO-ASA band-structure calculations. Differences in the phononic specific heat of the compounds result both from the different molar masses and the strong elongation of the lattice parameter c with the R-atom radii.

1. Introduction

The series of the ternary RAuGe (R = Sc, Y, La–Nd, Sm, Gd–Lu) intermetallic compounds [1–3] exhibits interesting structural and physical properties. The structures of these compounds are derived from the $CaIn_2$-type structure by an ordered arrangement of the gold and germanium atoms on the indium position. In a previous paper [3] we have shown by single-crystal structure refinements and TB-LMTO-ASA band-structure calculations that the degree of puckering of the [AuGe] hexagons depends significantly on the size of the rare-earth element. While the gold and germanium atoms form two-dimensional [AuGe] polyanions in CeAuGe [2, 3], a three-dimensional network of elongated tetrahedra is present in ScAuGe [3].

The physical properties of these germanides strongly depend on the nature of the rare earth element. ScAuGe and LuAuGe are diamagnets [3], whereas ferromagnetic ordering at 10 K was observed for CeAuGe [2]. GdAuGe orders antiferromagnetically at 14 K [4]. A detailed study of the (magnetic) specific heat, electrical resistivity, Hall effect, thermal conductivity and thermopower of these compounds will be reported in a forthcoming publication [4].

Here we report on the magnetic susceptibility, electrical resistivity and specific heat of ScAuGe, YAuGe, LaAuGe and LuAuGe, the compounds of the RAuGe series which have no

† New address: Anorganisch-Chemisches Institut, Universität Münster, Wilhelm-Klemm-Straße 8, D-48149 Münster, Germany.

0953-8984/97/071435+16$19.50

magnetic moment. In addition, the structures of YAuGe and LaAuGe have been refined from single-crystal x-ray data. The crystal structures of ScAuGe and LuAuGe have already been reported [3]. We discuss the measured electronic properties, i.e. the Pauli susceptibility χ_P, the Sommerfeld coefficient γ of the electronic specific heat and the temperature dependence of the electrical resistivity $\rho(T)$, in connection with the results of tight-binding LMTO-ASA band-structure calculations for all four compounds. The differences in the phononic specific heats of the RAuGe are analysed within Debye's theory.

2. Experimental details

The starting materials for the preparation of ScAuGe, YAuGe, LaAuGe, and LuAuGe were ingots of the rare-earth elements (Johnson–Matthey), gold wire (Degussa) and germanium lumps (Wacker), all with stated purity better than 99.9%. The rare-earth ingots were cut into small pieces in a dry box and kept under argon prior to the reactions. The samples ($\approx$1 g total mass) were prepared by arc melting of the elemental components in the ideal ratio in an argon atmosphere. The argon was purified by molecular sieves, a titanium sponge (at 900 K) and an oxysorb catalyst [5]. The melted buttons were turned over and each side was remelted several times to ensure homogeneity. The weight loss after melting was always smaller than 0.2%. The buttons were subsequently enclosed in evacuated silica tubes and annealed at 1070 K for ten days. They are light grey, stable in air and quite brittle.

Table 1. Lattice constants of hexagonal RAuGe compounds. The values marked with asterisks were obtained from high-angle reflections ($32^\circ < 2\Theta < 49^\circ$) on the four-circle diffractometer.

Compound	a (pm)	c (pm)	c/a	V (nm^3)	Reference
ScAuGe	430.82(5)	684.58(10)	1.589	0.1100(1)	[3]
YAuGe	441.00(3)	730.86(5)	1.657	0.1231(1)	This work
YAuGe*	440.91(3)	730.53(6)	1.657	0.122 99(2)	This work
YAuGe	440.8(3)	730.7(3)	1.658	0.1230(1)	[1]
LaAuGe	446.20(5)	816.05(8)	1.829	0.1407(1)	This work
LaAuGe*	445.87(3)	816.31(7)	1.831	0.140 52(2)	This work
LaAuGe	446.3(3)	816.9(3)	1.830	0.1409(1)	[1]
LuAuGe	437.75(4)	711.38(6)	1.625	0.1181(1)	[3]

In order to check the purity of our products, all samples were characterized through their x-ray powder diagrams using the modified Guinier technique [6] with Cu Kα_1 radiation and silicon ($a = 543.07$ pm) as an internal standard. All powder patterns showed single-phase samples. The lattice constants (see table 1) were refined from the powder data by least-squares fits. To assure correct indexing, the observed patterns were compared to calculated ones [7], using the atomic parameters from the structure refinements.

Magnetic susceptibilities were measured on polycrystalline pieces ($\approx$1 g) with a VTS SQUID magnetometer (SHE Incorporated) between 4.5 and 350 K at magnetic flux densities up to 4.0 T.

Electrical resistivity measurements of ScAuGe and LuAuGe were performed on small polycrystalline platelets ($\approx 1.5 \times 1.5 \times 0.5$ mm^3) with a dc four-probe set-up. The resistivities of larger bars of YAuGe and LaAuGe were measured in combination with the thermopower and thermal conductivity. The results of these measurements will be presented in a forthcoming publication [4].

The samples for heat capacity measurements (1–1.5 g) were mounted on the sapphire

sample holder of the calorimeter. The addenda heat capacity was measured separately and subtracted. We used the quasi-adiabatic step-heating method (Nernst's method) as described e.g. in [8]. The error of $c_p(T)$ between 1.7 and 50 K is $<2\%$.

Single-crystal intensity data were measured by use of a four-circle diffractometer (CAD4) with Ag Kα radiation and a scintillation counter with pulse-height discrimination.

Table 2. Technical data concerning the band-structure calculations (see the text).

	s	p	d	f	S (au)		s	p	d	f	S (au)
Sc	l	i	l		3.375	Y	l	i	l	i	3.643
Au	l	l	l	i	2.840	Au	l	l	l	i	2.848
Ge	l	l	l		2.807	Ge	l	l	l		2.819
E	l	l			1.728	E	l	l			1.737
La	l	i	l	l	4.123	Lu	l	i	l	l	3.524
Au	l	l	l	i	2.801	Au	l	l	l	i	2.862
Ge	l	l	l		2.772	Ge	l	l	l		2.832
						E	l	l			1.729

2.1. Electronic structure calculations

The electronic structures of all four compounds were calculated *ab initio* using the self-consistent TB-LMTO-ASA method [9]. A local exchange correlation potential was used [10] and all relativistic effects were included except for the spin–orbit coupling. The LMTO method has been described fully elsewhere [9, 11] and we shall therefore only give some technical data used for the calculations in table 2.

In this table the inclusion of a partial wave (s = angular momentum 0, p = angular momentum 1, and so on) in the LMTO basis set is indicated by an l (meaning low), and an included partial wave, which has been downfolded, is indicated by an i (meaning intermediate). S is the sphere radius in atomic units. E stands for interstitial spheres which had to be inserted in order to make the sum of the volumes of all of the spheres in the unit cell equal to the unit-cell volume. No overlap between two atomic-centred spheres exceeds 16% and the overlap between an atomic sphere and an interstitial sphere never exceeded 18%. The interstitial spheres were at the $\boldsymbol{a}/3 + 2\boldsymbol{b}/3$ equivalent positions, except for LaAuGe where no interstitial spheres were found necessary. The sphere radii and the positions of the interstitial spheres were determined by an automatic algorithm developed by Krier *et al* [12]

For ScAuGe and LuAuGe, the calculations were basically the same as in [3], except that we used 624 irreducible points in the tetrahedron k-space integration [13]. For YAuGe and LaAuGe we used 624 and 732 irreducible k-points, respectively.

3. Results and discussion

3.1. Structure refinements

Single crystals of YAuGe and LaAuGe were selected from the crushed buttons after the annealing process and investigated by Buerger precession photographs in order to check their symmetry and suitability for intensity data collection. The photographs showed hexagonal Laue symmetry, and the systematic extinctions (hhl was only observed with $l = 2n$, $00l$

Table 3. Crystal data and structure refinement for YAuGe and LaAuGe.

Empirical formula	YAuGe	LaAuGe
Formula weight	358.47 g mol^{-1}	408.47 g mol^{-1}
Temperature	293(2) K	293(2) K
Wavelength	56.086 pm	56.086 pm
Crystal system	Hexagonal	Hexagonal
Space group	$P6_3mc$	$P6_3mc$
Unit-cell dimensions	See table 1	See table 1
Formula units per cell	$Z = 2$	$Z = 2$
Calculated density	9.67 g cm^{-3}	9.64 g cm^{-3}
Crystal size	$25 \times 50 \times 50$ μm^3	$40 \times 50 \times 75$ μm^3
Absorption correction	From Ψ-scan data	From Ψ-scan data
Transmission ratio (max/min)	1:0.490	1:0.406
Absorption coefficient	51.29 mm^{-1}	41.59 mm^{-1}
$F(000)$	300	336
Θ range for data collection	4.0° to 30.0°	4.0° to 30.0°
Scan type	$\omega/2\Theta$	$\omega/2\Theta$
Range in hkl	±7, ±7, ±12	±7, ±7, ±14
Total number of reflections	1090	1092
Independent reflections	314 ($R_{\text{int}} = 0.0616$)	358 ($R_{\text{int}} = 0.0818$)
Reflections with $I > 2\sigma(I)$	285 ($R_{\text{sigma}} = 0.0362$)	291 ($R_{\text{sigma}} = 0.0612$)
Refinement method	Full-matrix least-squares on F^2	Full-matrix least-squares on F^2
Data/restraints/parameters	307/0/11	348/0/11
Goodness of fit on F^2	1.189	1.197
Final R-indices ($I > 2\sigma(I)$)	$R1 = 0.0256$, $wR2 = 0.0657$	$R1 = 0.0339$, $wR2 = 0.0711$
R-indices (all data)	$R1 = 0.0309$, $wR2 = 0.0693$	$R1 = 0.0450$, $wR2 = 0.0787$
Extinction coefficient	0.015(3)	0.006(2)
Largest diffraction peak and hole	1886 and -1550 electrons nm^{-3}	3914 and -2150 electrons nm^{-3}
Twin ratio (BASF)	0.66(7)	0.62(6)

Table 4. Atomic coordinates and isotropic displacement parameters (pm^2) for YAuGe and LaAuGe. U_{eq} is defined as one third of the trace of the orthogonalized U_{ij}-tensor. Asterisks indicate fixed parameters [17].

Atom	Wyckoff site	x	y	z	U_{eq}
YAuGe					
Y	2a	0	0	0.0342(2)	86(2)
Au	2b	1/3	2/3	0.25*	115(2)
Ge	2b	1/3	2/3	0.8250(3)	83(3)
LaAuGe					
La	2a	0	0	0.0096(3)	85(2)
Au	2b	1/3	2/3	0.25*	102(2)
Ge	2b	1/3	2/3	0.7773(3)	100(6)

only with $l = 2n$) led to the possible space groups $P6_3mc$, $P\bar{6}2c$, and $P6_3/mmc$, of which $P6_3mc$ (No 186) was found to be correct, in agreement with the earlier investigations [1–3]. Crystallographic data and some details of the data collections are summarized in table 3.

The structures were refined using the program SHELXL-93 [14] with anisotropic displacement parameters for all atoms. In both refinements the calculated FLACK

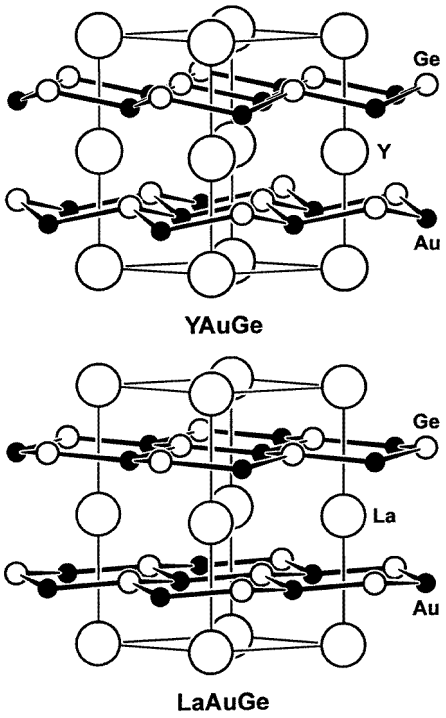

Figure 1. Crystal structures of YAuGe and LaAuGe. The strong Au–Ge intralayer bonds are indicated.

parameters [15, 16] had a value of about one half, indicating twinning by inversion. This was recently also observed for CeAuGe [2] and LuAuGe [3]. Therefore the inversion twin matrix ($\bar{1}00$, $0\bar{1}0$, $00\bar{1}$) was introduced and a batch scale factor (BASF) was refined. The refinements then converged to lower residuals and improved standard deviations. For the refinement of YAuGe, seven reflections with $F_o^2 < -2\sigma(F_o^2)$, and ten reflections for the refinement of LaAuGe were treated as unobserved. The final difference Fourier analyses were flat in both refinements. The highest residual peaks (see table 3) were too small and too near to the gold position (81 pm in YAuGe and 105 pm in LaAuGe) to be indicative of an additional atomic site. Most probably they resulted from an incomplete absorption correction of the data. Atomic parameters and interatomic distances are listed in tables 4 and 5. Listings of the structure factors and the anisotropic displacement parameters are available†.

The crystal structures (figure 1) of the ternary germanides RAuGe (R = Sc, Y, La, Lu) are derived from the well known $CaIn_2$-type structure [18] by an ordered arrangement of the gold and germanium atoms on the indium position. A detailed description of the crystal chemistry of these intermetallics was already given in [2, 3].

The gold and germanium atoms form puckered [AuGe] hexagons with very similar *intralayer* Au–Ge distances of 257.6 pm, 260.5 pm, 258.6 pm, and 260.5 pm in ScAuGe [3], YAuGe, LaAuGe, and LuAuGe [3]. These distances are significantly smaller than the

† They may be obtained from: Fachinformationszentrum Karlsruhe, D-76344 Eggenstein-Leopoldshafen, Germany. (Registry Nos: CSD-405323 (YAuGe) and CSD-405322 (LaAuGe).)

Table 5. Interatomic distances (pm) calculated with the lattice constants derived from x-ray powder data. All distances shorter than 530 pm (Y–Y, Y–Au, Y–Ge, La–La, La–Au, La–Ge) and 420 pm (Au–Au, Au–Ge, Ge–Ge) are listed. The standard deviations are all equal to or smaller than 0.2 pm.

	YAuGe				LaAuGe		
Y:	3	Ge	297.0	La:	3	Ge	319.9
	3	Au	299.5		3	Au	323.8
	3	Au	328.6		3	Au	333.5
	3	Ge	331.7		3	Ge	337.8
	2	Y	365.4		2	La	408.0
	6	Y	441.0		6	La	446.2
Au:	3	Ge	260.5	Au:	3	Ge	258.6
	3	Y	299.5		3	La	323.8
	1	Ge	310.6		3	La	333.5
	3	Y	328.6		1	Ge	385.8
Ge:	3	Au	260.5	Ge:	3	Au	258.6
	3	Y	297.0		3	La	319.9
	1	Au	310.6		3	La	337.8
	3	Y	331.7		1	Au	385.8

sum of the metallic radii of 281.1 pm [19] for Au and Ge for coordination number 12. The intralayer Au–Ge interactions are of strongly bonding character, as recently demonstrated by band-structure calculations [3].

The degree of puckering of the [AuGe] hexagons is strongly dependent on the size of the rare-earth atoms. While the layers are almost flat in the lanthanum compound, strong puckering is observed in the other three germanides. The decrease in the lattice parameter c with decreasing size of the rare-earth atom and the stronger puckering on going from the lanthanum to the scandium compound changes the dimensionality of the [AuGe] polyanion. In LaAuGe and YAuGe (*interlayer* Au–Ge distances of 385.8 pm and 310.6 pm, respectively), the [AuGe] polyanions are two dimensional and separated from each other. In LuAuGe the interlayer Au–Ge distance amounts to 292.7 pm, compatible with weak interactions between the layers. The transition from [AuGe] layers to a three-dimensional network of elongated tetrahedra then occurs for ScAuGe. There the Au–Ge interlayer distances of 275.2 pm are the shortest within the series of the RAuGe germanides. The structures of LaAuGe and YAuGe may therefore be described as of the NdPtSb type [20]. The structures of ScAuGe and LuAuGe are more closely related to that of LiGaGe [21, 22].

3.2. Electronic structure

The calculated electronic structures along some symmetry lines in the hexagonal Brillouin zone are shown in figure 2 for all four compounds. The electronic structures are similar. Only LaAuGe shows some small but important differences. The corresponding densities of states are shown in figure 3. The Ge s bands are situated at around -11 eV ($E_F = 0$ eV), except for for LaAuGe where they are lying about 1 eV higher in energy. The Au d bands are situated at around -6 eV and also these bands are about 1 eV higher in LaAuGe. For LuAuGe, the Lu f bands coincide with the d bands. The positions of these localized states are, however, not well determined in a local density calculation like the present one. The conduction bands extending from about -5 eV to the Fermi level comprise the six Ge p

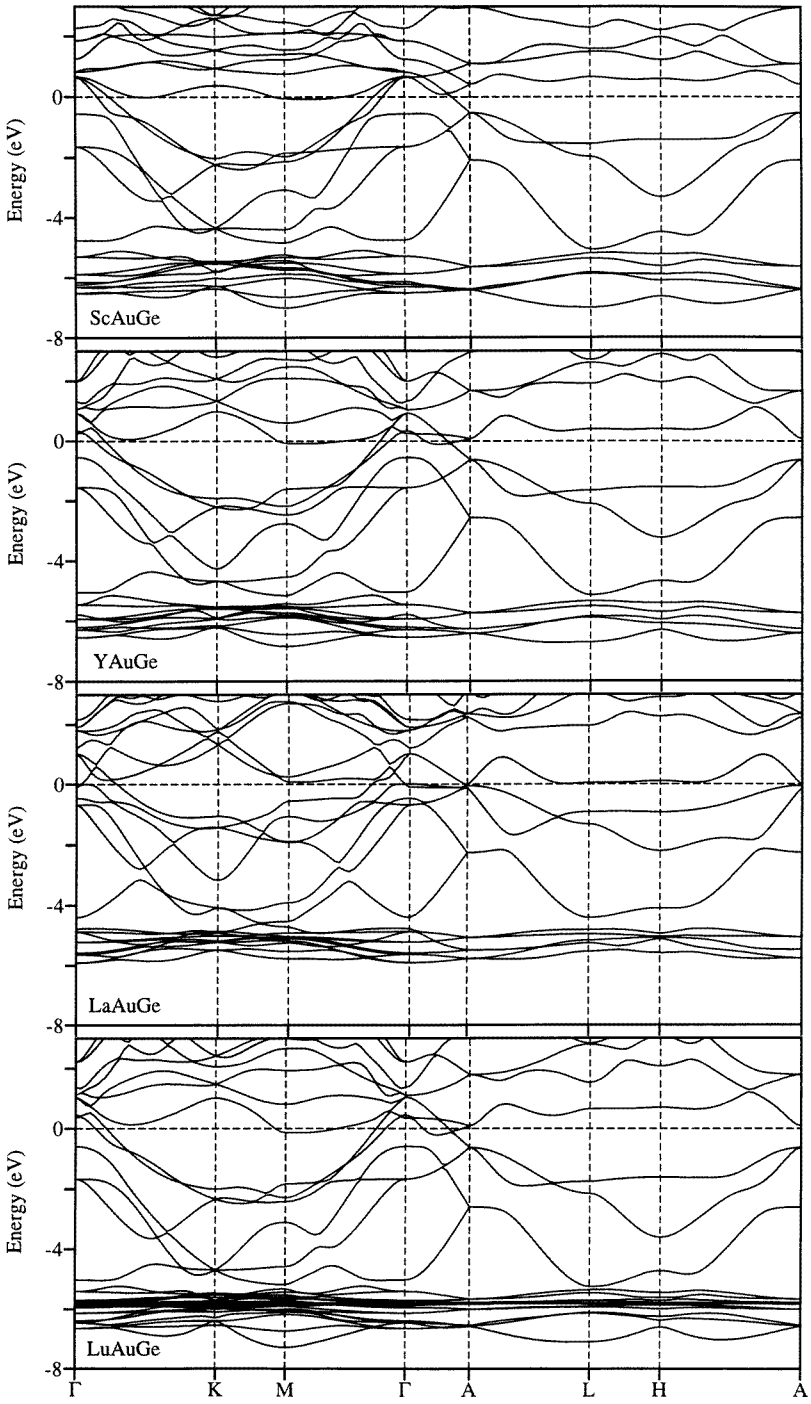

Figure 2. The self-consistent energy band structures of ScAuGe, YAuGe, LaAuGe, and LuAuGe along some symmetry lines in the hexagonal Brillouin zone. The zero of energy is at the Fermi level.

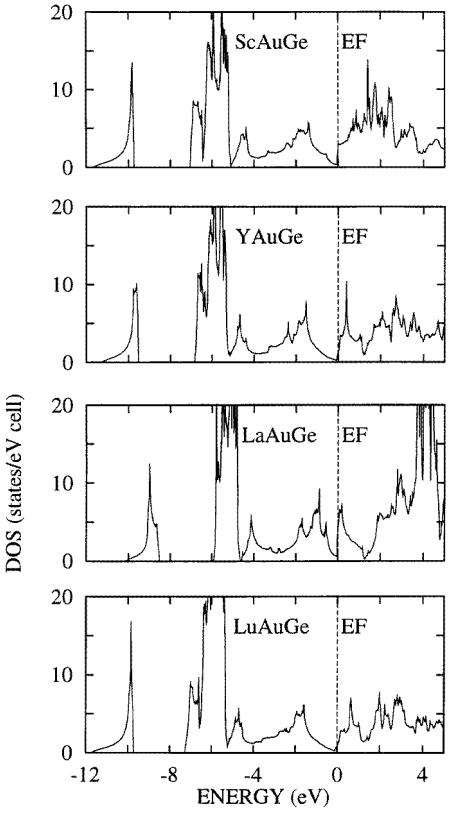

Figure 3. The self-consistent total densities of states of ScAuGe, YAuGe, LaAuGe, and LuAuGe. The zero of energy is at the Fermi level.

Table 6. Temperature-independent parts χ_0 of the magnetic susceptibilities of the compounds RAuGe as obtained from fits of the experimental data with equation (1). The diamagnetic increments for the R^{3+} ions χ_{inc}^{R} were taken from [25]. The Pauli paramagnetic susceptibility χ_P is obtained according to $\frac{2}{3}\chi_P = \chi_0 - \chi_{inc}^{R} - \chi_{inc}^{[AuGe]}$, taking into account the Landau electron diamagnetism with $\chi_L = -\frac{1}{3}\chi_P$. The term $\chi_{inc}^{[AuGe]} = -74(1) \times 10^{-6}$ emu mol^{-1} is the extrapolated increment for the [AuGe] polyanion (see the text and figure 6). The electronic densities of states N_F at E_F are given in states eV^{-1} for two spins and one formula unit: RAuGe.

	χ_0	χ_{inc}^{R}	χ_P	γ	N_F	χ_P/γ
R	(10^{-6} emu mol^{-1})			(mJ mol^{-1} K^{-2})	(eV^{-1})	($3(\mu_B/\pi k_B)^2$)
Sc	−38(2)	−6	63(4)	0.72(1)	1.4	6.4
Y	−56(1)	−12	45(3)	0.87(1)	0.6	3.8
La	−10(2)	−20	126(4)	2.50(2)	2.1	3.7
Lu	−78(1)	−17	20(3)	0.40(1)	0.4	3.6

states. They are nearly filled and, as a consequence, a pseudo-gap appears just below the Fermi level which stabilizes the structures. The lowest unoccupied bands are the Sc, Y, La, or Lu d bands. The densities of states at the Fermi level N_F are listed in table 6.

Even though the Fermi energies are determined very accurately numerically, with a large number of k-points, there is some uncertainty in these values. This is because of the steep slopes in the densities of states at the Fermi level which makes the size of N_F very sensitive to details in the chosen structural parameters or the local density parametrization. Both may lead to slight shifts of subbands relative to each other and therefore give rise to a small change in the Fermi level. That N_F is larger for LaAuGe than for the other compounds is, however, a consequence of the real structure. As may be seen in figure 2, the high value of N_F in this compound is due to the flat band right at the Fermi level and close to the L–H line. This La d band hybridizes strongly with the flat Ge p band at about -1 eV. The two bands therefore repel each other and this repulsion is smaller in LaAuGe than in the other three compounds because of the anomalously large c/a ratio in LaAuGe. This large c/a ratio is, of course, also found in CeAuGe [2, 4] and the following RAuGe compounds with large R atoms.

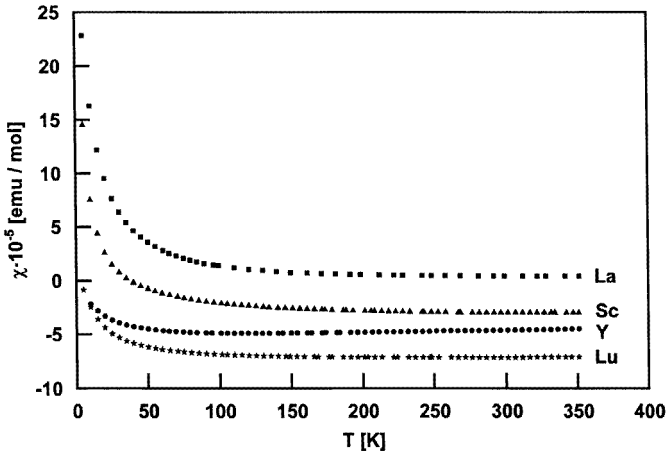

Figure 4. Magnetic susceptibilities of RAuGe compounds measured at 4 T.

3.3. The magnetic susceptibility and electronic specific heat

Figure 4 displays the molar magnetic susceptibility of RAuGe from 5 to 350 K measured at 4 T. A systematic increase of the room temperature susceptibilities in the series from LuAuGe via YAuGe and ScAuGe to LaAuGe is noticeable.

Below 50 K a Curie-like upturn is seen which can be accounted for by magnetic impurities in amounts ranging from 0.1% for YAuGe to 0.4% for LaAuGe of $S = 1/2$ species. Above 50 K, apart from YAuGe, all compounds exhibit an almost temperature-independent susceptibility. The susceptibility of YAuGe shows a weak linear increase with temperature.

Above 50 K the magnetic susceptibilities can be well fitted to

$$\chi(T) = C/T + \chi_0 + aT. \tag{1}$$

The Curie term C/T accounts for magnetic impurities. The temperature-independent part χ_0 (cf. table 6) is the sum of the diamagnetic susceptibility of the closed-shell and conduction electron contributions.

The fits reveal a coefficient a for the linear increase of the susceptibility which amounts to $2.6(2) \times 10^{-8}$ emu mol^{-1} K^{-1} for LaAuGe and YAuGe and of $1.2(2) \times 10^{-8}$ emu mol^{-1} K^{-1} for LuAuGe and ScAuGe. This increase, in the cases of ScAuGe, LaAuGe and LuAuGe, is masked by the Curie term arising from the magnetic impurities. The linear increase aT must be attributed to a temperature dependence of the conduction electron susceptibilities $\chi_P(T)$.

The temperature dependence of the Pauli susceptibility is determined by the first and second derivatives with respect to energy of the electronic density of states at the Fermi energy [23, 24]. High-temperature corrections to the Pauli susceptibility are frequently observed e.g. for the transition metals. For the RAuGe series they are positive and reach up to more than 20% of χ_0 in the case of YAuGe. We attribute this behaviour to a very structured electronic density of states in the neighbourhood of E_F, as is evident from our TB-LMTO-ASA band-structure calculations.

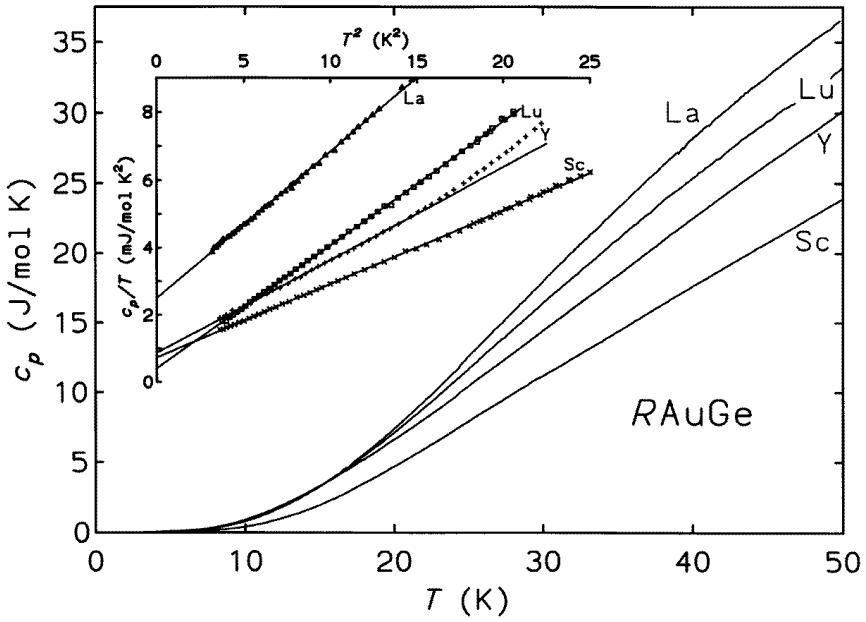

Figure 5. The specific heats $c_p(T)$ of the four RAuGe compounds. The insert shows a c_p/T versus T^2 plot for $T < 5$ K. The straight lines are least-squares extrapolations to $T^2 = 0$.

Figure 5 shows the specific heat $c_p(T)$ of the RAuGe from 1.7 K to 50 K. In the inset the low-temperature part of the measurements is displayed in a $c_p(T)/T$ versus T^2 representation. From the respective intercepts and the slopes of the straight lines fitted to these data the electronic specific heat coefficient γ (see table 6) and the initial Debye temperature $\Theta_D(0)$ (see table 7) are obtained. We note that YAuGe and LaAuGe show positive deviations from Debye's T^3-law above 4 K and ScAuGe and LuAuGe above about 5 K. The findings will be discussed in detail in section 3.5.

While ScAuGe, YAuGe and LuAuGe exhibit quite small electronic specific heat coefficients γ, LaAuGe has a markedly larger electronic term of 2.50(2) mJ mol^{-1} K^{-2}.

To extract χ_P from χ_0, knowledge of the diamagnetic increments is necessary. Diamagnetic increments $\chi_{inc}^{R^{3+}}$ are well known for the R^{3+} ions (cf. e.g. [25]). The dia-

Table 7. The molar mass M, and observed and calculated initial Debye temperatures $\Theta_D(0)$ of the four RAuGe compounds (see the text).

	M	$\Theta_D(0)$/K		
Compound	(g mol^{-1})	Observed	First scaling	Second scaling
ScAuGe	314.5	298.3	—	—
YAuGe	358.5	276.3	279.4	270.4
LaAuGe	408.5	237.7	261.8	239.7
LuAuGe	444.5	251.5	250.9	279.2

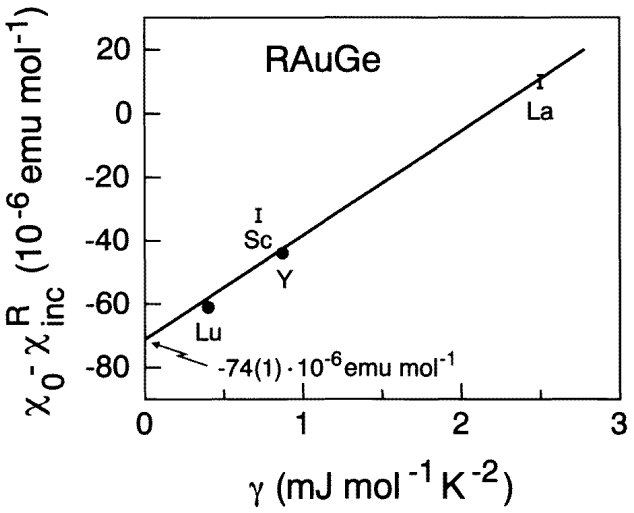

Figure 6. A plot of the temperature-independent part in the magnetic susceptibilities χ_0 corrected by the diamagnetic increments of the individual R^{3+} ions versus the electronic term γ in the heat capacity. The extrapolated diamagnetic increment of the [AuGe] polyanion is indicated.

magnetic increment $\chi_{inc}^{[AuGe]}$ for the complex polyanion [AuGe], however, is difficult to estimate from the tabulated increments for Au and Ge.

For an analysis of γ and χ_P, we therefore performed the following procedure. The fitted temperature-independent parts in the susceptibilities χ_0 were corrected by the tabulated increments for the R^{3+} ions $\chi_{inc}^{R^{3+}}$ and the difference is plotted versus γ (figure 6). As can be seen in figure 4, the differences $\chi_0 - \chi_{inc}^{R^{3+}}$ for YAuGe, LaAuGe and LuAuGe follow a linear relationship in γ,

$$\chi_0 - \chi_{inc}^{R^{3+}} = c\gamma + d \tag{2}$$

with $d = -74(1) \times 10^{-6}$ emu mol^{-1} and $c = 34(1) \times 10^{-6}$ emu mJ^{-1} K^{-2}.

The good correlation of the YAuGe, LaAuGe and LuAuGe data suggests that $\chi_{inc}^{[AuGe]}$ is identical for these compounds and amounts to $d = -74(1) \times 10^{-6}$ emu mol^{-1}. After correcting for the diamagnetism of the polyanion and for the Landau electron diamagnetism $\chi_L = -\frac{1}{3}\chi_P$ we finally obtain the electronic Pauli susceptibility χ_P (see table 6).

The ratio χ_P/γ (i.e. $\frac{3}{2}$ times the slope c in figure 6), within error bars, is identical for YAuGe, LaAuGe and LuAuGe. This so-called Wilson ratio is markedly enhanced over the value of unity expected for a Fermi–Sommerfeld free-electron gas model. Values of 3.6–3.8

are calculated for the three latter compounds, while for ScAuGe we obtain 6.4 (see table 6). Values three times larger than unity are frequently found for d-electron elements, as can be calculated from tabulated data, e.g. those given in [24]. Also in heavy-fermion systems, where γ may be several orders of magnitude larger than in our RAuGe, values of χ_P/γ larger than unity are found [26]. Exchange enhancement of the Pauli susceptibility, causing an increase of χ_P, and a low effective mass, leading to a decrease of γ, may account for this finding.

The Pauli susceptibility observed for ScAuGe is too high to fit into this scheme. The marked deviation may be attributed to a strong exchange enhancement of the susceptibility, but may, as well, indicate that the diamagnetic increment for the polyanion [AuGe] differs significantly from that of the three other compounds. In fact, only in the case of ScAuGe are strong interlayer bonds between Au and Ge atoms of neighbouring [AuGe] layers formed such that the polyanion changes its character giving rise to the smallest lattice parameter c observed in the RAuGe series (see table 1).

LaAuGe exhibits the highest values of γ and χ_P among the four compounds investigated. This correlates well with the largest density of states as found in the band-structure calculations. Values of N_F deduced from the γ-values are, however, only 20–60% of those obtained from the band-structure calculations, with the Sc compound showing the largest discrepancy. This implies that the effective electron mass in the RAuGe is smaller than one. On the other hand, values deduced from χ_P are consistently (40–130%) too high compared with those calculated from the band structure. Here YAuGe shows the strongest deviation.

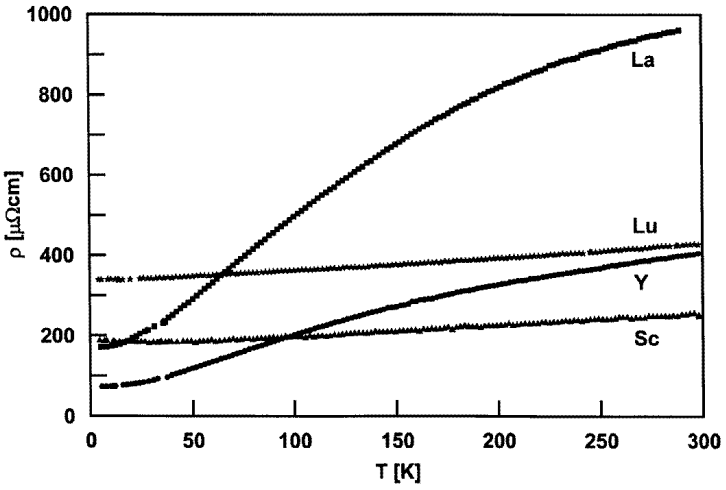

Figure 7. Electrical resistivities $\rho(T)$ of small irregular pieces of RAuGe. The error in ρ due to the geometry factor is $\pm 20\%$.

3.4. Electrical resistivity

In figure 7 we show the electrical resistivity $\rho(T)$ for the four compounds. Apart from the quite different residual resistivities ρ_0, which may in parts arise e.g. from microcracks of the brittle, polycrystalline buttons, two features are remarkable. First, the values of

$\rho(300\ \mathrm{K}) - \rho_0$ are very different for ScAuGe (63 $\mu\Omega$ cm) and LuAuGe (92 $\mu\Omega$ cm) on one hand, and for YAuGe (337 $\mu\Omega$ cm) and especially LaAuGe (804 $\mu\Omega$ cm) on the other hand. Second, the curvature of $\rho(T)$ is typically metal-like with a nearly linear slope at high temperatures for the compounds with lower $\rho(300\ \mathrm{K})$, while the $\rho(T)$ of YAuGe and especially LaAuGe show a tendency towards saturation at higher temperatures.

The large specific resistivity and the convex temperature dependence of $\rho(T)$ at high temperatures for LaAuGe (less pronounced for YAuGe) hint at an additional scattering mechanism, e.g. a narrow band near E_F [27]. For LaAuGe this is the scattering of the Ge p-band conduction electrons into a La d band which is flat near E_F in an extended part of the Brillouin zone (see section 3.2). A similar temperature dependence of $\rho(T)$ is also observed for CeAuGe [4].

3.5. Phononic properties

The main plot of figure 5 shows the specific heat $c_p(T)$ of the four RAuGe compounds from 1.7 to 50 K. In the inset, as discussed above, we display $c_p(T)/T$ versus T^2. The observed initial Debye temperatures $\Theta_D(0)$ resulting from the straight-line fits are listed in table 7. Note that the Y and La compounds show positive deviations from the simple Debye T^3-law starting at $\approx$4 K. For ScAuGe and LuAuGe, deviations become visible at temperatures above 5 K.

The initial Debye temperature $\Theta_D(0)$ depends strongly on the low-frequency (acoustic) phonons, i.e. vibrations of the heaviest atomic masses in the lattice in the direction of softest binding forces, which are activated at the lowest temperatures. $\Theta_D(0)$ for ScAuGe is the largest among those of the four compounds due to the small molar mass of ScAuGe.

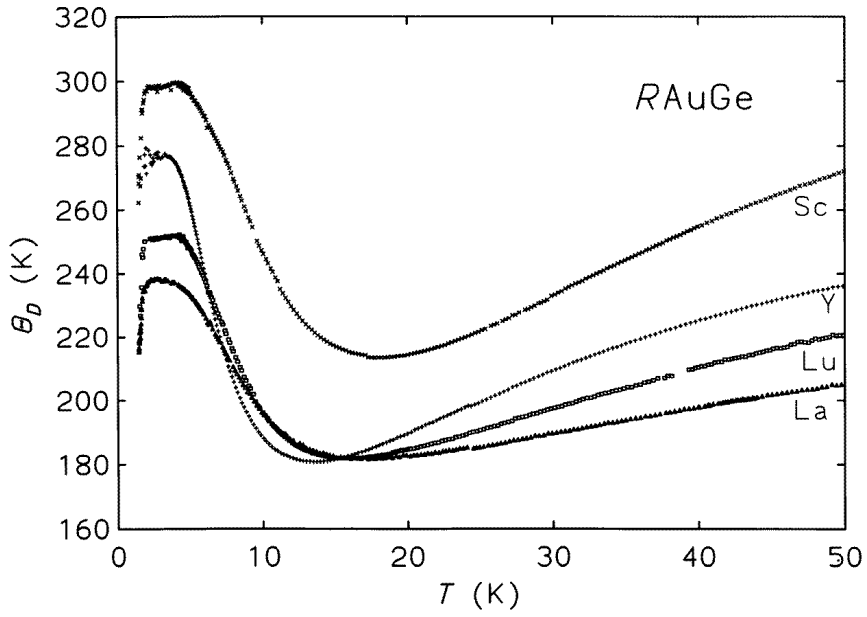

Figure 8. Equivalent Debye temperatures $\Theta_D(T)$ versus temperature (see the text) for the specific heats of the four RAuGe compounds.

In order to analyse $c_p(T)$ for the magnetic RAuGe compounds with R = Ce, ..., Yb we need reliable estimates for the phononic contribution of the individual RAuGe. This contribution, however, changes significantly with the lattice constant c, i.e. with the radius of the R atom. The situation for the 'non-magnetic' RAuGe is displayed in figure 8, where we plot the equivalent Debye temperatures $\Theta_D(T)$, as calculated by solving (by iteration) the equation $c_p(T) - \gamma T = N\mathcal{D}(\Theta_D(T)/T)$ for the lattice specific heat capacity. Here $\mathcal{D}$ denotes the Debye function [28] and $N = 3$ is the number of atoms/f.u. The curves $\Theta_D(T)$ decrease strongly from $\Theta_D(0)$, starting at around 4–5 K.

This 'softening' is particularly pronounced for YAuGe and relatively weak for LaAuGe, whereas the shapes of the curves of ScAuGe and LuAuGe are similar, due to their similar c/a ratio. All compounds have a minimum in $\Theta_D(T)$ at temperatures around 14–19 K ($\approx\Theta_D(0)/20$), which is typically observed in such plots [28]. At higher temperatures $\Theta_D(T)$ of all compounds increases. This 'hardening' is, as expected, stronger for the lighter compounds.

In order to understand the behaviour of $\Theta_D(T)$ of these structurally nearly identical compounds, we use a crude, simplified model. We treat the lattice as a harmonic oscillator with mass M and spring constant D. M represents the mass of the average atom, i.e. the molar mass. Then, $\Theta_D = \hbar\omega_D/k_B$ is proportional to $\sqrt{D/M}$.

First, we try a scaling of $\Theta_D(0)$ with $\sqrt{D/M}$, assuming at first a constant D. That may correspond to a constant strength of an interatomic binding force, determined preferentially by the interlayer Au–Ge bonding in the [AuGe] polyanions. The resulting values of $\Theta_D^R(0) = \Theta_D^{Sc}(0)\sqrt{M^{Sc}/M^R}$ scaled to $\Theta_D(0)$ for ScAuGe are given in table 7. This scaling works perfectly for LuAuGe and satisfactorily for YAuGe, while it fails for LaAuGe. It is surprising that the scaling of $\Theta_D(0)$ for ScAuGe works well for the heavy LuAuGe, but not for LaAuGe. This means that the average binding force for LaAuGe is significantly smaller than those of ScAuGe, LuAuGe, and YAuGe.

In fact, the structure of the [AuGe] polyanions changes from the 3D network to 2D layers stacked in the c-direction [3] in proceeding from ScAuGe to LaAuGe. We now assume (as a crude approximation) that the binding forces vary as $D \propto 1/c$. The lattice constant c is essentially determined by the distance between the [AuGe] layers. This second scaling, with $\sqrt{M^{Sc}c^{Sc}/M^Rc^R}$, yields better agreement with the experimental value of $\Theta_D(0)$ for LaAuGe.

The behaviour of $\Theta_D(T)$ near and above the temperature of the minima is also related to the change of the structure of the polyanions. ScAuGe (light constituent Sc, strong binding forces) has the largest Θ_D(50 K). LuAuGe is heavy and still 'hard', YAuGe is light, but the binding forces in the c-direction are considerably weakened, and LaAuGe is lighter than LuAuGe, but due to the 2D character it behaves in a very 'soft' manner.

These findings show that special caution is necessary in deducing the phononic contribution of $c_p(T)$ for RAuGe with R = Ce, ..., Yb, especially at elevated temperatures. Both mass and suitable lattice corrections have to be applied for the analysis of e.g. crystal-electric-field effects.

4. Conclusion

In summary, we have presented a comprehensive investigation of the structural and electronic properties of the non-magnetic members of the RAuGe family. The ratio c/a of the hexagonal lattice exhibits a remarkable large variation from ScAuGe ($c/a = 1.589$) to LaAuGe ($c/a = 1.830$) which leads to (i) a flattening of the [AuGe] polyanion a, b-layers and (ii) a decoupling of the [AuGe] polyanion layers in the c-direction.

The structural evolution from ScAuGe to LaAuGe results in a systematic trend in the electronic band structure as verified by TB-LMTO-ASA calculations. The Ge p bands are nearly filled and they are separated from the next unoccupied R d band by a pseudo-gap. Due to this pseudo-gap the electronic densities of states N_F at E_F are small for all four compounds, which is reflected in the Pauli susceptibilities χ_P and in the Sommerfeld coefficient γ of the specific heat. The small enhancement in the N_F of LaAuGe is due to a La d band right at E_F which also leads to a higher resistivity ρ(300 K) of LaAuGe with respect to the other RAuGe compounds. The ratio χ_P/γ is the same ($\approx$3.7) for YAuGe, LaAuGe, and LuAuGe.

The phononic properties (Debye temperature $\Theta_D(T)$) are determined in view of the application to the analysis of the specific heat of magnetic RAuGe compounds. They are governed by the structural trends as well as by the variation of the mass of the R atoms.

Acknowledgments

We are indebted to W Röthenbach for taking the Guinier powder patterns, to N Rollbühler for the resistivity measurements, to E Brücher for the susceptibility measurements and to Dr W Gerhartz (Degussa AG) for a generous gift of gold metal. The Stiftung Stipendienfonds des Verbandes der Chemischen Industrie supported our research by awarding a Liebig grant to RP.

References

[1] Rossi D, Marazza R and Ferro R 1992 *J. Alloys Compounds* **187** 267
[2] Pöttgen R, Borrmann H and Kremer R K 1996 *J. Magn. Magn. Mater.* **152** 196
[3] Pöttgen R, Borrmann H, Felser C, Jepsen O, Henn R, Kremer R K and Simon A 1996 *J. Alloys Compounds* **235** 170
[4] Bartkowski K, Schnelle W, Pöttgen R, Poddar A, Gibson B G, Gmelin E, Kremer R K and Simon A 1997 to be published
[5] Krauss H L and Stach H 1969 *Z. Anorg. Allg. Chem.* **366** 34
[6] Simon A 1971 *J. Appl. Crystallogr.* **4** 138
[7] Yvon K, Jeitschko W and Parthé E 1977 *J. Appl. Crystallogr.* **10** 73
[8] Gmelin E 1987 *Thermochim. Acta* **110** 183
[9] Andersen O K 1975 *Phys. Rev.* B **12** 3060
Andersen O K and Jepsen O 1984 *Phys. Rev. Lett.* **53** 2571
[10] von Barth U and Hedin L 1971 *J. Phys. C: Solid State Phys.* **4** 2064
[11] Andersen O K, Jepsen O and Glötzel D 1985 *Highlights of Condensed-Matter Theory* ed F Bassani, F Fumi and M P Tosi (New York: North-Holland)
[12] Krier G, Jepsen O and Andersen O K 1997 to be published
[13] Jepsen O and Andersen O K 1971 *Solid State Commun.* **9** 1763
Blöchl P E, Jepsen O and Andersen O K 1994 *Phys. Rev.* B **49** 16 223
[14] Sheldrick G M 1993 *SHELXL-93 Program for Crystal Structure Refinement* (University of Göttingen)
[15] Flack H D 1983 *Acta Crystallogr.* A **39** 876
[16] Bernadinelli G and Flack H D 1985 *Acta Crystallogr.* A **41** 500
[17] Schwarzenbach D, private communication (Lausanne)
Due to the small number of parameters an automatic restraint of the floating origin is not possible.
[18] Iandelli A 1964 *Z. Anorg. Allg. Chem.* **330** 221
[19] Teatum E, Gschneidner K A Jr and Waber J 1960 *US Department of Commerce (Washington, DC) Report* LA-2345
[20] Wenski G and Mewis A 1986 *Z. Kristallogr.* **176** 125
[21] Bockelmann W, Jacobs H and Schuster H-U 1970 *Z. Naturf.* b **25** 1305
[22] Bockelmann W and Schuster H-U 1974 *Z. Anorg. Allg. Chem.* **410** 233
[23] Ashcroft N W and Mermin N D 1976 *Solid State Physics* (New York: Holt, Rhinhart and Winston)
[24] Shimizu M, Takahashi T and Atsushi K 1962 *J. Phys. Soc. Japan* **17** 1740

Shimizu M, Takahashi T and Atsushi K 1963 *J. Phys. Soc. Japan* **18** 240
[25] Selwood P W 1956 *Magnetochemistry* (New York: Interscience)
[26] Lee P A, Rice T M, Serene J W, Sham L J and Wilkins J W 1986 *Comment. Condens. Matter Phys.* **12** 99
[27] Gratz E and Zuckermann M J 1982 *Handbook of the Physics and Chemistry of Rare Earth* ed K A Gschneidner Jr and L Eyring (Amsterdam: North-Holland) ch 42
[28] Gopal E S R 1966 *Specific Heat at Low Temperatures* (London: Plenum)